ISSN 2070-2051, Protection of Metals and Physical Chemistry of Surfaces, 2022, Vol. 58, No. 3, pp. 453–461. © Pleiades Publishing, Ltd., 2022.
Russian Text © The Author(s), 2022, published in Fizikokhimiya Poverkhnosti i Zashchita Materialov, 2022, Vol. 58, No. 3, pp. 252–261.

PHYSICOCHEMICAL PROCESSES AT THE INTERFACES

Physicochemical and Adsorption Properties of Some Carbon Materials in Aqueous Solutions

N. A. Skorik[a], *, T. S. Kharlamova[a], E. N. Vostretsova[a], and N. N. Dyukarev[a]

[a] *National Research Tomsk State University, Tomsk, 634050 Russia*

**e-mail: skorikninaa@mail.ru*

Received April 28, 2021; revised January 30, 2022; accepted January 30, 2022

Abstract—Water dispersions of carbon adsorbents—nanodiamonds of UD-DP and UD-HP-DP types, nanodiamond charge of UDB-A type, C_{60} fullerene, nanotubes, and activated carbon—were studied. Some physicochemical properties of their surface (acidity and electrokinetic characteristics) were investigated, and the surface values of pK_{a1} were calculated. The data on adsorption of iodine, malic acid, and cationic dyes onto these adsorbents from aqueous and 1 mol/L NaCl solutions were discussed and compared. The dye-adsorption data and the values of the ζ potential and suspension effect indicated a negatively charged surface of UDA-SP nanodiamond within a pH adsorption range from 5.5 to 8.0.

Keywords: adsorption, carbon materials, UDD, ζ potential, iodine, malic acid, cationic dyes

DOI: 10.1134/S2070205122030212

INTRODUCTION

In recent years, carbon nanomaterials (CNMs) such as nanodiamonds (ND) and fullerenes, carbon nanotubes (CNTs), and graphene and its derivatives, carbon materials (CMs), such as activated carbons (ACs), have been widely used as adsorbents. In the reviews [1, 2], consideration was given to the current state of CNMs and to their use in water treatment and the removal of mercury from wastewaters, as well as their industrial applications.

THEORETICAL ANALYSIS

Nanodiamonds are a type of carbon nanomaterials with a large number of functional groups on their surface, making them suitable for modification. Thus, NDs modified with ionic liquids showed high removal efficiency (92.8%) of Congo red dye from an aqueous solution [3]. The adsorption capacity of carboxyl groups-modified detonation-synthesized nanodiamonds (DNDs) dispersed in aqueous solutions is three times higher than that of unmodified DNDs with respect to nitrate ions and metal cations (Cu^{2+} and Pb^{2+}) [4]. However, the practical application of nanodiamonds is limited by their poor dispersive ability in water.

Fullerenes have high chemical stability, and they can interact with the cellular environment and pass through cell membranes to deliver therapeutic molecules [5]. An innovative synthesis of a magnetic fullerene nanocomposite was proposed [6], and the mechanism of adsorption of methylene blue and Acid Blue 25 anionic dyes onto it was attributed mainly to electrostatic, π-π stack interactions, and hydrogen bonds.

In work [7], the synthesis of an adsorbent with magnetic multi-walled CNTs was suggested, and their adsorption properties in the context of the effective removal of health-hazardous mycotoxin were described. The removal of phenol and crystalline violet dye from the solution by means of modified CNTs was studied [8]. The work [9] provided an overview of the processes of adsorption of heavy metals from water using carbon nanotubes.

Low-cost activated carbons, most often nonnanomaterials, are widely used. Activated carbon prepared from sewage sludge is an efficient and stable adsorbent for the removal of metals from aqueous media [10]. Activated carbon modified with multiwalled CNTs showed a high adsorption capacity in removing humic acids [11]. Improved adsorption of copper(II) ions on modified activated carbons in the presence of amino groups was demonstrated [12]. Efficient adsorption of methylene blue was achieved using cork and paper-waste-based activated carbons (with a high specific surface area of 1670 m^2/g) [13].

The ζ potential is one of the most significant features of aqueous colloids and suspensions. Knowing its magnitude and its sign, one can understand the mechanism of adsorption. Thus, the antibacterial activity of low-molecular-weight products of chitosan (LMWCs) was associated mainly with the difference in the ζ potential between the surface of LMWC particles and the bacteria [14]. The high adsorption capacity in respect to anionic dyes onto colloid parti-

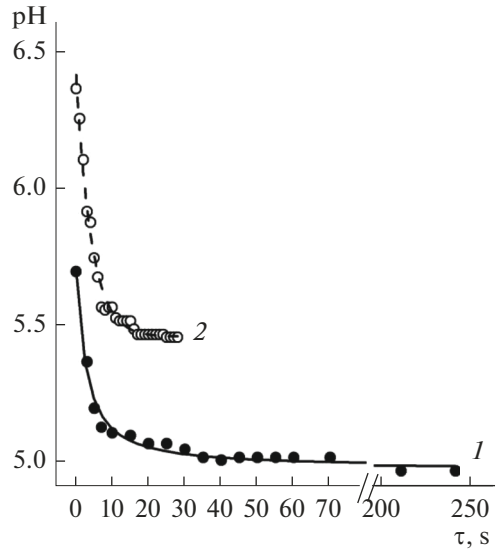

Fig. 1. Changes in pH over time in the following systems. (*1*) Fullerenes–H_2O (0.025 g fullerenes, 5 mL H_2O); results of calculations: $R^2 = 0.991$, $pH_0 = 4.96 \pm 0.01$, $= 5.69$, $= 5.69$, $pK_1 = 4.23$. (*2*) UD-DP–H_2O (0.05 g UD-DP, 10 mL H_2O); results of calculations: $R^2 = 0.988$, $pH_0 = 5.45 \pm 0.01$, $pH^{in}_{exp} = 6.36$, $pH^{in}_{calc} = 6.41$, $pK_1 = 4.49$.

cles was attributed to the positive sign of the ζ potential of their aggregates [15]. It was assumed that a partially positively charged amino group of glycine contributed to adsorption onto the surface of CNTs at pH 6 ($\zeta_{CNT} < 0$) [16]. In the process of electroflotation extraction of AC particles of grade OU-B from solutions, the most effective surfactants are cationic and nonionic types, and the surfactants of anionic type are ineffective, which is explained by the negative value of the electrokinetic ζ potential of carbon particles [17].

The destruction of adsorbent aggregates is usually carried out using physical methods: ultrasonic treatment, centrifugation, filtration or by inserting counterions. The ζ potential is a measure of the electrostatic (repulsion/attraction) interactions between particles, and it is also one of the major parameters affecting the stability of dispersed systems. Measurements and data on the magnitude and sign of the ζ potential provide a new insight to and allow better control of the mechanism of disintegration. As a result, both the stability and the storage period of the system can be increased.

Thus, the invention [18] relates to a method of obtaining a ζ-negative dispersion of carboxylated nanodiamonds (the ζ potential is more than −35 mV at pH >7). Pluronic F-127 (nonionogenic surfactant) was used to prepare concentrated aqueous suspensions of carbon nanotubes that remained stable during long-term storage (for more than 4 years) [19]. In [20], the nature of the negative charge of particles and the reasons for the aggregate stability of fullerene dispersions were discussed. Typically, nanoscale fullerene aggregates in polar solvents are negatively charged, which is caused by the selective adsorption of OH^- ions on the surface of C_{60}.

The purpose of the present work is to study and compare the physicochemical properties of the surface of some carbon materials and their adsorption activity in respect to inorganic and organic substances.

MATERIALS AND METHODS

In the present work, we studied CNMs produced by S&P CJSC SINTA: DNDs of UD-DP and UD-HP-DP types, nanodiamond charge of the UDB-A type, and fullerene C_{60}. We also used carbon nanotubes and pharmacopeial AC of Medisorb type; the malic acid and dyes used were analytical grade reagents. Measurements of the ζ potential were carried out at room temperature in automatic mode using an Omni S/N analyzer (Brookhaven, United States); the specific surface areas of the CNT and AC samples were evaluated by the BET method from the low-temperature nitrogen adsorption isotherm measured on a 3Flex Surface Characterization Analyzer. Electronic absorption spectra of solutions were recorded using a LEKISS 2107UV spectrophotometer; the optical density was also measured on a KFK-2-UHL 4.2 photoelectrocolorimeter with absorption layer thickness $l =$ 10 mm. The pH values in solutions were measured using a pH-meter of pH-673 type, a glass electrode of which was calibrated using buffer solutions with pH ranged from 3.56 to 6.86.

EXPERIMENTAL

Investigation of Aqueous Suspensions of CM

The acidity of the surface of the adsorbents was investigated using the kinetic method according to the method described in [21]. The acid–base parameter of the surface, which is the pH of the isoionic state pH_0, was evaluated from the kinetic curves of the pH–τ dependence (τ is time) for an aqueous suspension of samples of nanocarbon adsorbents and activated carbon after equilibrium has been established. Figure 1 shows the kinetic curves for the adsorbents, the pH value of which is below the initial pH of water (UD-DP, F), whereas Fig. 2 demonstrates that, for adsorbents with a pH above the initial pH of water (AC and UDB-A), an increase in the time of contact of the studied samples with water up to 1 h or more results in little to no further changes in pH of the suspension.

Investigation of the Electrokinetic Potential of CNMs in Aqueous Dispersions as a Function of pH

To measure the ζ potential, we prepared suspensions of the test sorbents with different pH values. To this end, a weighed portion of the adsorbent was added

to 5 mL of a 0.01 mol/L solution of H^+, K^+ (NO_3^-, OH^-). To achieve equilibrium, the suspension was shaken for 5 h, kept for 20 h, and subjected to ultrasonic exposure for 3 min in water at ambient temperature. Then, a well-suspended middle fraction (~1.5 mL) was taken with a pipette and placed into a measuring cell, after determining the ζ potential, the pH of the suspension was measured. Figure 3 shows the dependences of the ζ potential on the pH of suspensions of the (a) UD-DP nanodiamonds, (b) CNTs, and (c) UDB-A nanodiamond charge. The values of the ζ potential used are the average of the results of three measurements.

Below are the results of measurements of the ζ potential of fullerene (0.002 g in 5 mL of its suspension) at several values of pH:

pH_{susp}	2.01	3.43	5.77
ζ(average), mV	+10.29	−15.74	−26.03

Adsorption of Iodine, Dyes, and Malic Acid onto Several CNMs and ACs

When studying adsorption, we added a certain amount of adsorptive with a known concentration of adsorbed substances to a weighed portion of the adsorbent in a glass-stoppered flask; then, the mixture was shaken for 5 h and incubated for 20 h in the dark. After pH measurements of the resultant suspension, the mixture was centrifuged (3400–4000 rpm) for 30 min. Next, the optical density of adsorbate was measured and the nonadsorbing substance was determined. The value of adsorption a, mmol/g, was calculated by the formula

$$a = \left\{\left(C^0 - [C]\right)V\right\}/m,$$

where V is the volume of an adsorbate, m is the weight of an adsorbent, and C^0, $[C]$ are the initial and equilibrium concentrations of a substance in solution. Using the value of specific surface area of adsorbent s (for UD-DP and UDB-A, the values of s were taken from the certificates: 295 and 404 m^2/g, respectively; for CNTs and AC, the values of s were measured at the Tomsk State University Common Use Center: 703 and 400 m^2/g, respectively). Adsorption per adsorbent mass a, mmol/g, was recalculated to adsorption per unit of its surface area (a, μmol/m^2, Tables 1, 5).

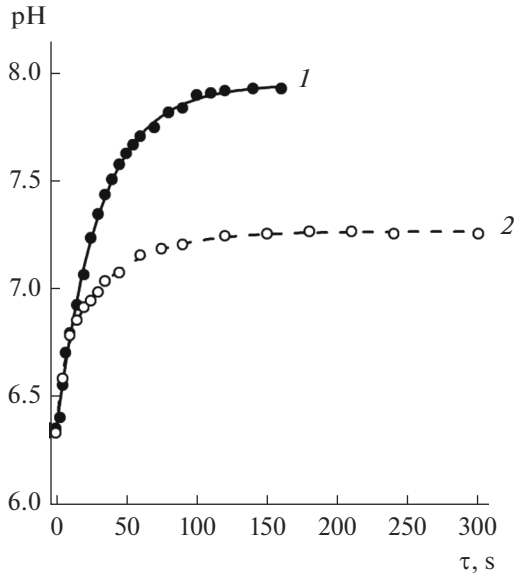

Fig. 2. Changes in pH over time in the following systems. (*1*) AC–H_2O (0.05 g AC, 10 mL H_2O); results of calculations: $R^2 = 0.998$, $pH_0 = 7.95 \pm 0.06$, $pH^{in}_{exp} = 6.36$, $pH^{in}_{calc} = 6.33$, $pK_{a1} = 9.57$. (*2*) UDB-A–H_2O (0.05 g UDB-A, 10 mL H_2O); results of calculations: $R^2 = 0.981$, $pH_0 = 7.25 \pm 0.01$, $pH^{in}_{exp} = 6.36$, $pH^{in}_{calc} = 6.41$, $pK_{a1} = 8.09$.

The adsorption of iodine and water-soluble dyes is a sensitive method for studying the surface of an adsorbent. The iodine adsorption was studied on UD-DP, UDB-A, and fullerene C_{60}. According to GOST (State Standard) 6217-74, the adsorption activity of activated carbon for iodine is determined using sodium thiosulfate to find the iodine content in an equilibrium adsorptive. We have developed a photometric method for determining iodine in an aqueous solution at λ = 540 nm. The equilibrium concentrations of iodine in the adsorbate (Table 1) were calculated taking into account the dependence of the optical density of the iodine solution on the pH value. For this purpose, we measured D_{540} for the iodine solutions ($C(I_2) = 2.35 \times 10^{-3}$ mol/L), in which pH values were within a pH range of equilibrium solutions of the iodine solution–adsorbent system:

D_{540}, nm	0.228	0.236	0.271	0.287	0.290
pH	2.7	3.4	3.8	5.6	5.2

Table 1. Data on iodine adsorption onto different adsorbents ($C^0(I_2) = 2.45 \times 10^{-3}$ mol/L, $V(I_2) = 6$ mL, $m_{ads\text{-}t} = 0.05$ g)

Adsorbent	pH_{susp}	D_{540}, nm	$[I_2]$, mol/L	a, mmol/g // a, μmol/m^2
UD-DB	3.45	0.220	2.19×10^{-3}	0.031 // 0.11
UDB-A	5.80	0.046	3.77×10^{-4}	0.250 // 0.62
Fullerene	2.82	0.051	5.26×10^{-4}	0.232

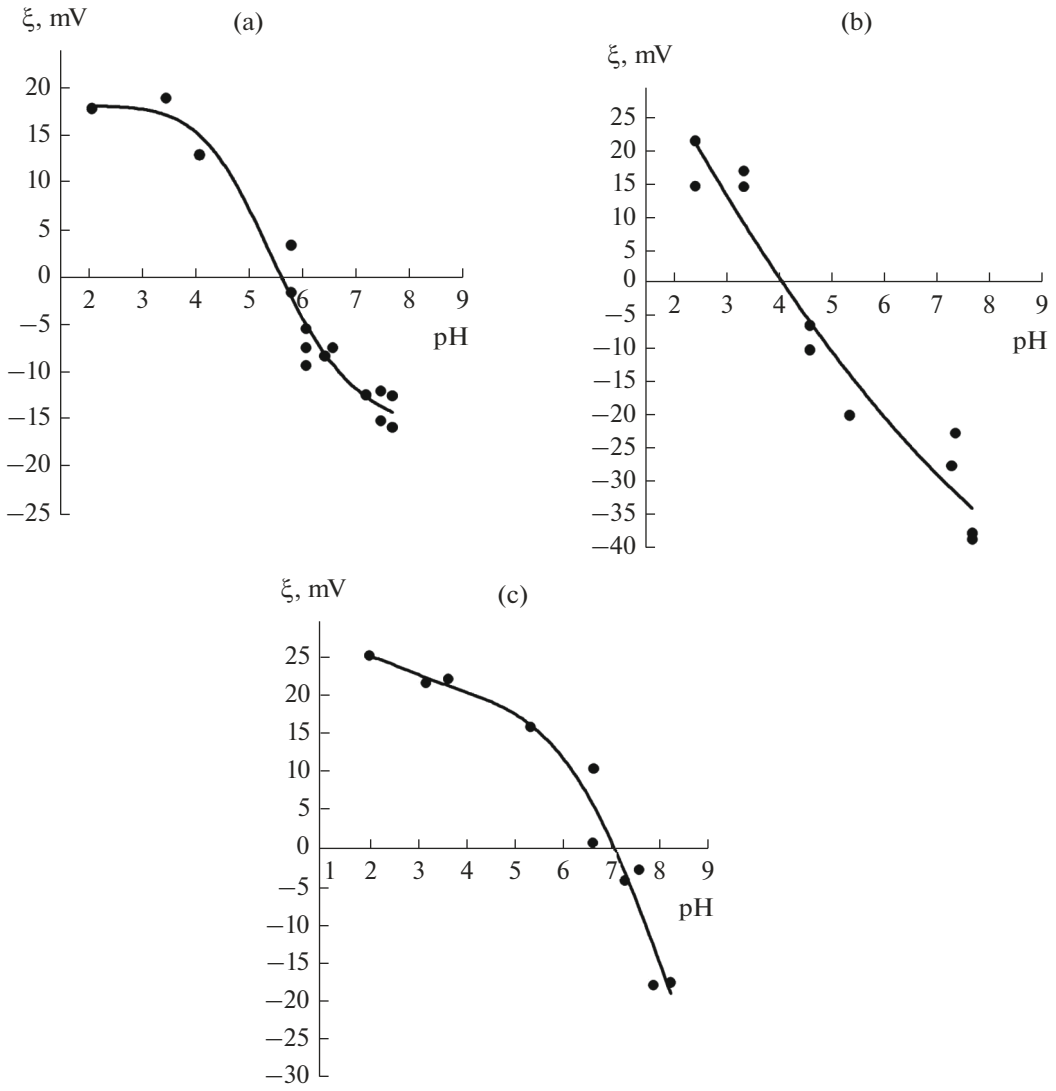

Fig. 3. The dependence of the ζ potential of the surface of particles on the pH value of suspension: (a) UD-DP (m_{UD} = 0.01 g, d_{part} ≈ (300–800) nm), R^2 = 0.949; (b) CNT (m_{CNT} = 0.001 g, d_{part} ≈ (300–800) nm), R^2 = 0.936; and (c) diamond charge of UDB-A type ($m_{UDB\text{-}A}$ = 0.001 g, d_{part} ≈ (200–800) nm), R^2 = 0.897.

Specified dependence $D(I_2) = f(\text{pH})$ was approximated by the linear equation $y = 0.020x + 0.176$ (R^2 = 0.898). After determining $D_{540} = f(\text{pH})$, the iodine concentration was calculated using a proportion, since it was previously shown that at pH ≈ const Beer's law was obeyed within the range of iodine concentration of 8.15×10^{-4}–2.45×10^{-3} mol/L. Dependence $D(I_2) = f(C(I_2))$ was approximated by the linear equation $y = 117.3x - 0.0014$, R^2 = 0.980.

The adsorption of cationic type dyes—malachite green $[C_{23}H_{25}N_2]^+Cl^-$ (MG) and methylene blue $[C_{16}H_{18}N_3S]^+Cl^-$ (MB)—was studied on the UD-DP, UDB-A, and AC adsorbents in water and a 1 mol/L NaCl solution. Preliminary experiments have shown that the optical density of methylene blue and malachite green was almost constant over the pH range of 4.50–7.50 (see Table 2); therefore, the concentration of dyes in the equilibrium solution was determined using calibration curves $D = b + aC$ (for MB at λ = 540 nm, R^2 = 0.999, a = 6301, b = –0.066; at λ = 670 nm, R^2 = 0.987, a = 2563, b = 0.084; for MG at λ = 670 nm, R^2 = 0.998, a = 25342, b = –0.036). At a high adsorptive density (the UD-DP–MB system, λ = 540 nm), it was preliminary diluted. The working wavelength was selected according to the electronic absorption spectra, which are similar in shape for both dyes.

Table 3 lists the results of adsorption of the dyes in water and in a 1 NaCl mol/L solution onto different adsorbents.

Table 2. Dependence of optical density of indicators on pH ($C_{MB} = 6.82 \times 10^{-5}$ mol/L, $C_{MG} = 1.67 \times 10^{-5}$ mol/L, $l = 10$ mm)

pH		4.50	5.50	6.00	6.50	7.00	7.50
Methylene blue	D_{540}	0.351	0.351	0.350	0.352	0.353	0.350
Malachite green	D_{670}	0.368	0.365	0.366	0.367	0.368	0.365

Table 3. Adsorption of methylene blue and malachite green dyes onto different adsorbents in water and a 1 NaCl mol/L solution ($C^0_{MB} = 5.00 \times 10^{-4}$ mol/L, $C^0_{MG} = 5.00 \times 10^{-5}$ mol/L, $V_{sol} = 10$ mL, $m_{adsorb} = 0.05$ g)

Dye	Medium	Adsorbent	pH_{susp}	λ, nm	D	$[C]_{MB,MG}$, mol/L	a, mmol/g	Adsorption, %
MB	H_2O	UD-DP	5.50	540	0.498	2.69×10^{-4}	0.0462	46.2
		UDB-A	7.00		Turbid centrifugalized deposit			
		AC	6.66					
	1 M NaCl	UD-DP	5.40	670	0.282	7.72×10^{-5}	0.0846	84.6
		UDB-A	7.94		0.00	–	–	~100
		AC	7.45		0.00	–	–	~100
MG	H_2O	UD-DP	6.65	670	0.114	5.93×10^{-6}	0.0088	88.1
		UDB-A	7.4–7.8		Turbid centrifugalized deposit			
		AC	7.45		0.00	–	–	~100
	1 M NaCl	UD-DP	6.52	670	0.00	–	–	~100
		UDB-A	7.90–8.61		0.00	–	–	~100
		AC	7.47–7.57		0.00	–	–	~100

Table 4 summarizes the data on the adsorption of the dyes depending on pH of the medium (different pH values in the initial dye adsorbate were adjusted by HCl and NaOH solutions).

The adsorption of malic acid $C_4H_6O_5$ onto the UD-DP nanodiamond, UDB-A, and AC was studied under static conditions.

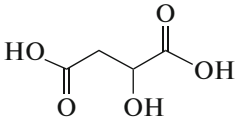

H_2Malat

In the equilibrium adsorptive, the concentration of the malate anion was determined from its absorption at λ = 440 nm using the calibration characteristics ($R^2 = 0.950$). The measurement error of the adsorption value of the malate ion was ~5–7%. Table 5 summarizes the data on adsorption of malic acid onto the specified adsorbents.

RESULTS AND DISCUSSION

Carbon materials—ultradispersed diamond powders of UD-DP, UD-HP-DP, and UDB-A; powders of carbon nanotubes; and fullerene C_{60}, activated car-

Table 4. Composition of equilibrium adsorbate, the value of adsorption in the systems MB–H_2O–UD-DP and MG–H_2O–UD-DP ($C^0_{MB} = 2.4 \times 10^{-4}$ mol/L, λ = 540 nm; $C^0_{MG} = 1.48 \times 10^{-5}$ mol/L, λ = 490, 540 nm; $V = 10$ mL. $m_{UDD} = 0.05$ g)

Methylene blue			Malachite green		
pH	[MB], mol/L	a_{MB}, mmol/g	pH	[MG], mol/L	a_{MG}, mmol/g
3.30	1.81×10^{-4}	0.0118	2.13	1.15×10^{-5}	0.0007
5.40	8.05×10^{-5}	0.0319	5.51	6.22×10^{-6}	0.0017
5.53	8.00×10^{-5}	0.0320	5.70	6.00×10^{-7}	0.0028
6.50	2.41×10^{-5}	0.0430	6.04	3.40×10^{-7}	0.0029

Table 5. Data on the adsorption of malic acid onto different adsorbents (V^0_{adst} = 10 mL; m_{adsrb} = 0.05 g; $C^0(H_2Malat)$ = 3.200×10^{-3} mol/L, $pH^0 = 2.86$)

Adsorbent	Characteristics of equilibrium adsorbate		a_{Malat}, mmol/g// a_{Malat}, μmol/m^2
	pH_{susp}	C_{Malat}, mol/L	
UD-DP	2.96	2.849×10^{-3}	0.070 // 0.24
UDB-A	3.34	1.386×10^{-3}	0.363 // 0.89
AC	3.74	1.231×10^{-3}	0.394 // 0.99

Table 6 pH values of the isostate (pH_0, pH_{IEP}) of water suspensions and pK_{a1} of the surface of carbon materials

No	CM	pH_0 values of suspensions, calculated pK_{a1}			pH_{IEP}
		R^2	pH_0	pK_{a1}	
1	UD-DP (different batches)	0.990 0.985 0.990	5.57 ± 0.01 5.45 ± 0.01 5.52 ± 0.01	4.39 4.49 5.26	5.5 5.6 –
	UD-HP-DP	0.998	5.61 ± 0.01	4.57	~6.3
2	Fullerines	0.991	4.96 ± 0.01	4.23; 3.5 [27]	~3
3	CNT	–	(5.5–6.3) [26]	–	4.2
4	UDB-A (batch no 4 and 5)	0.981	7.25 ± 0.01	8.09	7.1
		0.996	7.63 ± 0.03	8.72	–
5	AC (different batches)	0.998	7.95 ± 0.06; 7.9 [24]	9.56	–
		0.982	7.22 ± 0.02	8.67	
		0.999	7.34 ± 0.02	9.03	

bon of Medisorb type—exhibit adsorption activity due to the large specific surface ~(300–700 m^2/g) and functional surface cover, as well as the presence of various macro- and microdefects. In the present work, the data of approximation of the kinetic curves pH_{susp}–τ (Figs. 1, 2) were used to evaluate the pH_0 values of the isoionic state of the adsorbents and calculate pK_{a1} for the dominant functional groups of their surface. Then, dependence $\zeta = f(pH)$ for the suspensions of UD-DP, UD-HP-DP, fullerenes, CNTs, and UDB-A were employed to calculate the values of the surface isoelectric state pH_{ies} (Table 6).

It follows from Table 6 that the pH values of isoionic (pH_0) and isoelectric (pH_{IEP}) states for UDB-A (pH_0 7.3, pH_{IEP} 7.1) and UD-DP (pH_0 ~5.5, pH_{IEP} 5.5) are close, which may indicate the absence of specific adsorption of background electrolyte ions. During adsorption in solutions of indifferent electrolytes, the positions of pH_0 and pH_{IEP} coincide [22].

If the initial pH value of the dispersive medium (water) is $pH_{init} > pH_0$, then the kinetic curves pH–τ are located below the level of neutrality (Fig. 1); when $pH_{init} < pH_0$ (Fig. 2), they are above the level of neutrality. Under the condition of $pH_0 < pH_{susp}$, the surface of the particles is negatively charged (there are acid sites on the surface of the adsorbent), and, if $pH_0 > pH_{susp}$, the surface has a positive charge (there are basic sites on the surface of the adsorbent). This conclusion is confirmed by the dependence of the ζ potential on pH for the suspensions of UD-DP, CNTs, and UDB-A (see Fig. 3). The acid groups of the surface include, first of all, carboxyl and phenolic groups, the basicity of the carbon surface can be caused by, for example, surface nitrogen-containing groups. Using the Hammett indicator method, we have shown that there are sites of both acidic and basic types on the surface of UD-DP [23]. The pH_0 values for the suspensions of activated carbons of various types [24, 25]—7.9, 7.93, 8.66, and 7.95—are consistent with the values of 7.2–7.9 that we found. The pH_0 values for carbon nanotubes and nanoflakes in the 10^{-3} mol/L electrolyte solutions are within a range of 5.5–6.3 [26], which is comparable with the values of pH_0 determined in this work for suspensions of nano-

diamonds (5.5–5.6) and fullerenes (5.0). The surface of these adsorbents is dominated by acidic active sites of medium strength (pK_{a1} 4.2–5.3). In [27], it is indicated that there are groups with pK_a 3.5 on the surface of C_{60} fullerene. The surface groups with pK_{a1} of 3.5–6.0 can be assigned to carboxyl groups. Weak basic sites (pK_{a1} 8.1–9.6) dominate on the surface of adsorbents UDB-A (pH_0 7.3–7.6) and AC (pH_0 7.2–8.0).

The similarity of carbon adsorbents is associated not only with the structure of their surface, the nature and density of functional groups, the specific surface area, and the (sp^2, sp^3) state of carbon atoms, but also with the pK_{a1} values for dominant surface groups and ζ potentials. For the synthesized micro- and mesoporous activated carbons, pK_a values of 3.78, 6.38, and 8.17 were found, which correspond to carboxyl, lactonic, and hydroxyl groups, respectively [28]. It was found in [29] that, in the synthesis of carbon sorbents, the original activated carbon of BAC-A brand contained three types of acid sites with pK_a 4.35, 7.3, and 9.59. We found that the surface of the pharmaceutical AC under investigation contained functional groups with pK_a values within a range of 9.0–9.7, which determines the basicity of this adsorbent.

The electrokinetic potential determining the aggregate stability of suspension was found for the powders of UD-DP, UD-HP-DP, fullerenes, CNTs, and UDB-A at different pH values. It follows from Fig. 3 that, at pH 2–8, the values of electrokinetic potential were found to lie in the interval of approximately +20...–35 mV. The mechanism of particle surface charging can be attributed to the ionization of surface functional groups due to the changes in the pH of the solution. The increase in the negative value of the ζ potential with an increase in the pH of the medium was caused by the presence of surface functional groups of a predominantly acidic character. The pH_{IEP} value of 4.2 that we obtained for CNTs is close to that reported in [30]. According to the results of [31], the minimum values of the ζ potential for five types of powders were in the pH range of 5.5–7.5, and for those used in our work were in the range of 5.5–6.3.

Solutions of test compounds—iodine and water-soluble cationic dyes (MB and MG)—were used to study the adsorption properties of CMs. It is seen from Table 1 that the adsorption activities of UDB-A and fullerenes with respect to iodine (0.250 and 0.232 mmol/g) are comparable to each other, but they are higher than that of UD-DP with respect to the same substance (0.031 mmol/g). Our results are consistent with the states of atoms, which are close for the used carbon materials—UDB-A and fullerene-containing nondiamond sp^2-carbon (UDB-A comprises 40–60% of nondiamond sp^2-carbon), which is more reactive compared to the diamond phase (sp^3-carbon) in UD-DP. The adsorption activity of fullerene, in addition to the presence of nondiamond sp^2-carbon, is caused by the absence of orientation restrictions of adsorptive molecules in respect to the spherical fullerene molecules. The specific surface of the nanodiamond charge (404 m^2/g) exceeds that of nanodiamonds (295 m^2/g), which also contributes to its increased adsorption capacity compared to that of UD. Thus, it was shown in work [32] that the sorption capacity of the diamond charge for certain influenza A and B is higher than that of nanodiamonds. UDB-A, fullerenes, and UD-DP adsorbents are inherently hydrophobic, which suggests that the mechanisms of iodine adsorption have common features: dispersion interactions are realized between these adsorbents and iodine molecules.

Adsorption of ions is a more complex process than molecular adsorption; it is most often selective, i.e., cations and anions are adsorbed differently onto this adsorbent [33]. The electrostatic attraction between surface groups of CM and functional groups of substances in a solution is the most frequently proposed mechanism of the adsorption process, although other mechanisms are also suggested. When malic acid is adsorbed on UD-DP, UDB-A, and AC (Table 5), the initial adsorbate has a pH of 2.86. It follows from the yield diagram of malic acid (Fig. 4) that, at this pH, the adsorbate contains the H_2Malat (~65%), $HMalat^-$ (~35%), and $Malat^{2-}$ (~0%) particles. The adsorption of $HMalat^-$ malic-acid anions is possible on the positively charged basic site, whereas H_2Malat molecules can adsorb on the hydrophobic parts of carbon adsorbents. Since the surface of the adsorbents carries a positive charge at pH ~ 3, then the adsorption of H^+ ions is almost absent. This fact is confirmed by the negligible difference between pH_{susp} 2.96 of the UD-DP and pH 2.86 of the initial adsorbate; for the systems with UDB-A and AC, the differences between pH_{susp} and pH 2.86 are greater—3.34 and 3.74, respectively—and the adsorbent–solvent interaction process is also superimposed. According to Table 5, the adsorption activities of UDB-A and AC with respect to the H_2Malat, $HMalat^-$, and $Malat^{2-}$ particles of malic acid (the latter appears with increasing pH 2.86 of the initial adsorbate) are comparable with each other (0.363 and 0.394 mmol/g) and higher than the adsorption activity of UD (0.070 mmol/g).

In the case of colored cations R^+ of the MG $[C_{23}H_{25}N_2]^+$ and MB $[C_{16}H_{18}N_3S]^+$ dyes ($RCl \leftrightarrow R^+ + Cl^-$), the adsorption proceeds on the available active sites on the surface of the carbon material, with these sites being predominantly acidic and negatively charged. With an increase in the pH of the adsorptive, the surface of UD-DP acquires an increasingly negative charge, therefore, the sorption of the cationic MG and MB dyes increases (Table 4). A high percentage of sorption of MG and MB cationic dyes onto UD-DP, UDB-A, and AC within a pH range of 5.5–8.6 indi-

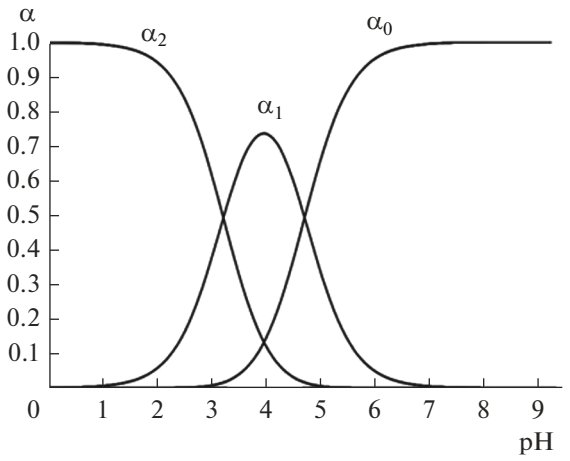

Fig. 4. Distribution of molecular and ionic forms of malic acid vs. pH value: α_2, H_2Malat; α_1, $HMalat^-$; and α_0, $Malat^{2-}$ ($C(H_2Malat) = 0.01$ mol/L, $\lg B_1 = 4.71$, $\lg B_2 = 7.93$).

cates a negatively charged surface of the adsorbents, which is also confirmed by the sign of the ζ potential of UD-DP and UDB-A within this pH interval (Figs. 3a, 3c). It follows from Table 3 that the value of sorption of dyes increased when passing from water to a 1 mol/L NaCl solution. An increase in ionic strength usually leads to a decrease in the adsorption of dyes probably due to the competition between their ions and NaCl ions for adsorption sites on the surface of the adsorbent. However, sometimes this pattern is violated. A growth of adsorption with an increase in ionic strength is associated with an intensification of the aggregation of certain dyes in solution. A similar aggregation process takes place on the surface of the adsorbent itself [34]. At a high ionic strength, there is a salting-out effect from a solution of salts with voluminous ions such as dyes.

Data on the sorption of cationic dyes, measurements of the ζ potential and suspension effect (Table 7) indicate a negatively charged surface of UD-DP nanodiamond within a pH range of 5.5–8.5 of sorption processes. The suspension effect (SE), which is numerically expressed by the ratio $\Delta pH = pH_{susp} - pH_{cf}$, manifests itself in the fact that the powder and the centrifugalized deposit of the same suspension have different pH values. In this case, the sign of SE coincides with the sign of the charge of the dispersed phase.

Table 7. Changes in the pH value of the UD-DP–H_2O suspension ($V(H_2O)$ = 10 mL; m_{UDD} = 0.05 g) upon centrifugation

$pH(H_2O)$	pH_{susp}	pH_{cf}	ΔpH
6.13	5.25	5.59	−0.34
6.44	5.51	5.73	−0.22
6.35	5.46	5.61	−0.15

CONCLUSIONS

1. Based on the data on the change in the pH of the suspension over time under nonequilibrium conditions of contact of the surface of UD-DP, UD-HP-DP, diamond charge UDB-A, fullerenes, and AC with water, we determined a measure of the acidity of their surface characterized by pH value of the isoionic state pH_0 and strength of acid–base sites pK_{a1}.

2. The electrokinetic characteristics of the samples of UD-DP, UD-HP-DP, CNT, diamond charge UDB-A, and fullerenes at pH 2–8 are within a range of approximately +20...–35 mV, for these adsorbents, the $\xi = f(pH)$ dependence was employed to determine the pH value of the isoelectric state of the surface pH_{IEP} at which the ξ potential is equal to zero.

3. When the acid–base equilibrium in the system is established, the pH values of the isoionic state pH_0 of the water suspensions of UD-DP and UDB-A (5.57 and 7.25) are close to the pH values of the isoelectric state pH_{IEP}: ~5.5 and 7.1, respectively. This fact makes it possible to estimate the absence of specific adsorption of ions of background electrolyte.

4. It was established that the adsorption activities of UDB-A and fullerenes, which contain nondiamond sp^2-carbon, in respect to iodine (0.250 and 0.232 mmol/g) are comparable to each other and higher than the adsorption activity of UD-DP (sp^3-carbon) with respect to this substance (0.031 mmol/g). The adsorption values of malic acid, which contains ions and molecules, onto UDB-A and AC are comparable to each other and higher than the adsorption value onto UD-DP.

5. A high degree of extraction of MB and MG dyes (85–100 and 100%) on the UD-DP, diamond charge UDB-A, and AC adsorbents with an increase in the ionic strength of the solution can be associated with the enhancement of the aggregation of dye in the solution and on the adsorbent or the salting-out effect of the salts with voluminous ions.

6. Data on the sorption of cationic dyes onto UD-DP, the results of measurements of the ζ potential and suspension effect indicate a negatively charged surface of nanodiamond UD-DP within a pH range of 5.5–8.5.

REFERENCES

1. Gusain, R., Kumar, N., and Ray, S.S., *Coord. Chem. Rev.,* 2020, vol. 405, p. 213111. https://doi.org/10.1016/j.ccr.2019.213111
2. Gupta, N.K. and Gupta, A., *FlatChem,* 2018, vol. 11, p. 1. https://doi.org/10.1016/j.flatc.2018.11.002
3. Guang Yang, Hongye Huang, Junyu Chen, et al., *J. Mol. Liq.,* 2019, vol. 296, p. 111874. https://doi.org/10.1016/j.molliq.2019.111874

4. Dolenko, T.A., Burikov, S.A., Laptinskiy, K.A., et al., *J. Alloys Compd.,* 2014, vol. 586, no. 1, Suppl., p. S436. https://doi.org/10.1016/j.jallcom.2013.01.055
5. Kazemzadeh, H. and Mozafari, M., *Drug Discovery Today,* 2019, vol. 24, no. 3, p. 898. https://doi.org/10.1016/j.drudis.2019.01.013
6. Elessawy, N.A., El-Sayed, E.M., Ali, S., et al., *J. Water Process Eng.,* 2019. https://doi.org/10.1016/j.jwpe.2019.101047. Elessawy, N.A., El-Sayed, E.M., Ali, S., et al., *J. Water Process Eng.,* 2020, vol. 34, p. 101047. https://doi.org/10.1016/j.jwpe.2019.101047
7. Zhuo Zhang, Chen Zeng, and Bangzhu Peng, *Food Control,* 2019, vol. 102, p. 1. https://doi.org/10.1016/j.foodcont.2019.02.038
8. Lawal, I.A., Lawal, M.M., Azeez, M.A., and Ndungu, P., *J. Mol. Liq.,* 2019, vol. 288, p. 110895. https://doi.org/10.1016/j.molliq.2019.110895
9. Fiyadh, S.S., AlSaadi, M.A., Jaafar, W.Z., et al., *J. Cleaner Prod.,* 2019, vol. 230, p. 783. https://doi.org/10.1016/j.jclepro.2019.05.154
10. Loretta, Y., Li Xu, Dong Gong, and Otman Abada, *Waste Manage.,* 2019, vol. 87, p. 375. https://doi.org/10.1016/j.wasman.2019.02.019
11. Noorimotlagh, Z., Ravanbakhsh, M., Valizadeh, M.R., et al., *Polyhedron,* 2020, vol. 179, p. 114354. https://doi.org/10.1016/j.poly.2020.114354
12. Mahaninia, M.H., Rahimian, P., and Kaghazchi, T., *Chin. J. Chem. Eng.,* 2015, vol. 23, no. 1, p. 50. https://doi.org/10.1016/j.cjche.2014.11.004
13. Novais, R.M., Caetano, A.P.F., Seabra, M.P., et al., *J. Cleaner Prod.,* 2018, vol. 197, p. 1137. https://doi.org/10.1016/j.jclepro.2018.06.278
14. Li-Chen Chen, Shao-Kai Kung, Hui-Huang Chen, and Shih-Bin Lin, *Carbohydr. Polym.,* 2010, vol. 82, no. 3, p. 913.
15. Kamneva, N.N., *Cand. Sci. (Chem.) Dissertation,* Kharkiv, 2015.
16. Manilo, M.V., *Nanosist., Nanomater., Nanotekhnol.,* 2015, vol. 13, no. 1, p. 25.
17. Davydkova, T.V., Kolesnikov, V.A., Milyutina, A.D., and Kolesnikov, A.V., *Khim. Bezop.,* 2019, vol. 3, no. 1, p. 96. http://chemsafety.ru. https://doi.org/10.25514/CHS.2019.1.15007.
18. Myullyumyaki, V. and Syuren, I., RF Patent 2015145029, 2017.
19. Parveen, S., Rana, S., Fangueiro, R., and Paiva, M.C., *Powder Technol.,* 2017, vol. 307, p. 1.0002681615.
20. Mchedlov-Petrosyan, N.O., *Khim., Fiz. Tekhnol. Poverkhn.,* 2010, vol. 1, no. 1, p. 19.
21. Skorik, N.A., Krivozubov, A.L., Karzhenevskii, A.P., and Spitsyn, B.V., *Prot. Met. Phys. Chem. Surf.,* 2011, vol. 47, no. 1, p. 54.
22. Ikonnikova, K.V., Ikonnikova, L.F., Minakova, T.S., and Sarkisov, Yu.S., *Teoriya i praktika pH-metricheskogo opredeleniya kislotno-osnovnykh svoistv poverkhnosti tverdykh tel* (Theory and Practice for pH-Metrical Determining Acid-Alkali Properties of Solid's Surfaces), Tomsk: Tomsk Polytechnic Univ., 2011.
23. Skorik, N.A., Vostretsova, E.N., and Nam, A.V., *Prot. Met. Phys. Chem. Surf.,* 2020, vol. 56, no. 1, p. 19.
24. László, K., Tombácz, E., and Novák, Cs., *Colloids Surf., A,* 2007, vol. 306, nos. 1–3, p. 95.
25. Khokhlova, T.D. and Le Thi Hien, *Moscow Univ. Chem. Bull.,* 2007, vol. 62, no. 3, p. 128.
26. Milyutina, A.D. and Kolesnikov, V.A., *Usp. Khim. Khim. Tekhnol.,* 2016, vol. 30, no. 3, p. 19.
27. Shirinkin, S.V., Volkova, T.O., and Nemova, N.N., *Meditsinskie nanotekhnologii. Perspektivy ispol'zovaniya fullerenov v terapii organov dykhaniya* (Medical Nanotechnologies. Trends for Applying Fullerenes for Therapy of Respiratory Organs), Petrozavodsk: Karelian Scientific Center Russ. Acad. Sci., 2009, p. 63.
28. Bikmukhametova, R.R. and Sharov, A.V., *Vestn. Kurgan. Gos. Univ. Khim. Nauki,* 2016, no. 4, p. 61.
29. Sharov, A.V., Bikmukhametova, R.R., Filisteev, O.V., et al., *Sorbtsionnye Khromatogr. Protsessy,* 2015, vol. 15, no. 2, p. 243.
30. Barany, Sh., Kartel', N., and Meszaros, R., *Colloid J.,* 2014, vol. 76, no. 5, p. 509.
31. Bazalii, G.A., in *Porodorazrushayushchii i metalloobrabatyvayushchii instrument - tekhnika i tekhnologiya ego izgotovleniya i primeneniya. Sbornik nauchnykh trudov* (Rock-Destruction and Metal-Processing tool – Technique and Technology for its Manufacturing and Applying. Collection of Scientific Works), Kyiv, 2013, issue 16, p. 329.
32. Ivanova, V.T., Ivanova, M.V., Burtseva, E.I., et al., *Vopr. Virusol.,* 2012, vol. 57, no. 2, p. 9.
33. Peristyy, A., Paull, B., and Nesterenko, P.N., *Adsorption,* 2016, vol. 22, no. 3, p. 371.
34. Giles, C.H. and D'Silva, A.P., *Trans. Faraday Soc.,* 1969, vol. 65, no. 9, p. 2516.

Translated by E. Khozina